

Determination of Captopril using platinum coated nanoporous gold film electrode

Nahid Tavakkoli*, Nasrin Soltani, Arezou Afsharpour

Chemistry Department, Payame Noor University, 19395-4697 Tehran, Iran

Received: 27 July 2015, Accepted: 22 February 2016, Published: 1 October 2016

Abstract

In this article electrochemical determination of captopril at the surface of the platinum coated nanoporous gold film (PtNPGF) electrode is reported using the cyclic voltammetry and amperometry. For the preparation of PtNPGF, the surface of NPGF electrode was covered with Cu layer using underpotential electrochemical deposition (UPD). Afterward, the copper layer is replaced with platinum ions via a spontaneous redox reaction to have a uniform Pt overlayer. Under the optimized conditions, the amperometry peak current of captopril increased linearly with captopril concentration in the ranges of 4.70×10^{-8} to 4.57×10^{-5} mol L⁻¹. The detection limit of captopril was 1.2×10^{-8} mol L⁻¹. The results show a very good precision (R.S.D < 2.4%), suitable selectivity and very stable response for captopril. The proposed sensor was successfully applied for the determination of captopril in the urine samples of patient human.

Keywords: Nanoporous, under potential deposition, platinum, Captopril.

Introduction

Captopril (CAP) belongs to a group of anti-hypertensive drugs that affects the renin-angiotensin system and is commonly referred to as angiotensin-converting enzyme (ACE) inhibitors.

The chemical name of captopril is (S)-1-(3-mercapto-2-methyl-L-oxopropyl)-L-proline and it is widely used for the treatment of arterial hypertension. Recent studies suggest that it may also act as a scavenger of

*Corresponding author: Nahid Tavakkoli

Tel: +98 (913)1296838, Fax: +98 (313)7381002
E-mail: Nahidtavakkoli2015@gmail.com

free radicals because of its thiol group [1, 2]. Several methods have been proposed for the determination of captopril, including high-performance liquid chromatography with pre- or post-column derivatization[3]colorimetry[4], fluorometry[5], chemiluminescence[6], capillary electrophoresis [7], spectrometry [8] and amperometry[9]. One of the important limits of liquid chromatography with UV detection is that captopril does not have sufficient absorption so a pre- or post-column derivatization procedure is normally required and this leads to increasing cost and complication of analysis. Electrochemical techniques are an alternative method for the captopril determination which is simple, fast and low cost. The electrochemical detection of captopril by using graphite [10] and selective membrane electrode[11] as the working electrode has been reported.

The nanoparticles have attracted great interests due to their extraordinary properties, such as small size and surface effects. Among them, noble metal nanoparticles, especially gold nanoparticles, were received intensive scientific and technological attentions

as they have unique electrical, optical and chemical properties.

Recently, nanoporous gold films (NPGFs) have been widely used in areas such as chemical or biochemical sensors and catalysis [12]. One important property of the NPGF is their higher surface area and better electron transport with respect to traditional gold nanoparticle modified electrodes. Like graphite electrodes, surface roughness helps exposing active sites of the NPGFs for fast electron transfer, as observed on graphite electrodes [13].

The ultra thin metal overlayers is a class of thin layer structures which has increasing applications in the fields of catalysis and fuel cells [14]. The physical and chemical behavior of ultra thin metal overlayers is different due to the difference of structural and electronic effects that dominates their properties [15, 16]. In the case where a ligand (substrate) effect is weak, the energy of the d-band center of ultra thin metal multilayers is predominantly affected by the level of consistent strain [16]. Pt adlayers on noble-metal surfaces is interesting because of unique film-dependent properties which are not normally observed in the bulk material [17]. Particularly, they exhibit

enhanced catalytic activity for a number of reactions, such as the anodic oxidation of small molecules (methanol, formic acid, and carbon monoxide) and the reduction of molecular oxygen [18, 19].

The fabrication of sub-monolayer or monolayer of Pt on Au affords a very high surface area to volume ratio, and thus provides a promising path to construct electrocatalysts with high specific activity (activity per unit weight) and high catalyst utilization in a controlled way. In fact, the ultimate goal for the development of these new catalysts is to reach 100% Pt utilization, in which every Pt atom on the electrode becomes available and catalytically active for the electrochemical reactions [20]. The ability of such Pt-Au catalysts has been the subject of some intensive researches. Improving the catalytic performance and utilization efficiency of Pt-based electrocatalysts can reduce the cost of sensors and thus speed up the commercialization of such sensors.

An underpotential deposition (UPD) is the electrochemical deposition of a (sub) monolayer of foreign metal ions onto a metal substrate where its potential is more positive than Nernst potential. The key question in the study

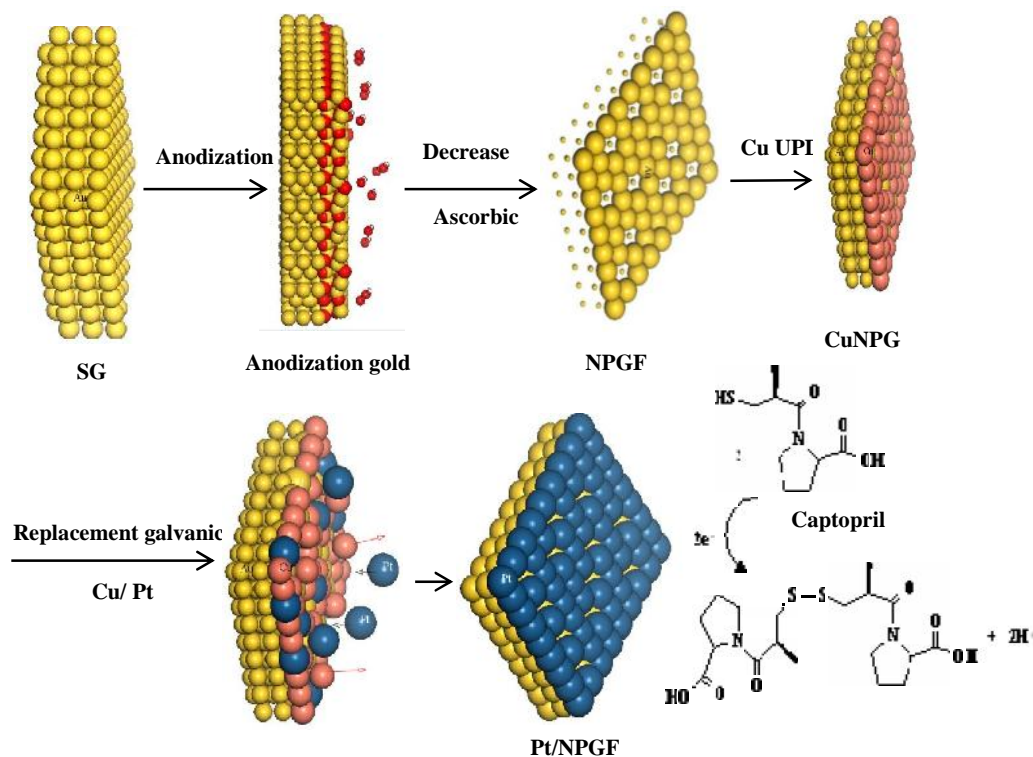
of UPD processes at the electrode-electrolyte interface addresses the correlation of the catalytic activity and selectivity of adatom-modified surfaces with the adlayer structure and the nature of adatoms. Recently, Cu UPD on platinum single crystals has been interesting for interfacial electrochemistry [21, 22].

It has been shown that metallic UPD adlayers can change the composition and chemical properties of an electrode surface. Metallic UPD would allow the precise and reproducible control of the surface coverage and the study of coverage dependent properties, including the structure of the metallic adlayer and its electronic properties [23]. The speed of electrochemical deposition on the surface of nanoporous substrate at thermodynamic potential varies at different sites, resulting in undesirable coating coverage. Metallic electrochemical deposition through UPD can form a nearly uniform layer of deposited metal.

In this work the surface of NPGF electrode was covered by a Cu layer to obtain UPD. Then UPD copper was replaced with platinum ions via a spontaneous redox reaction which

yielded a uniform Pt overlayer. The electrocatalytic activity of Pt/NPGF electrode for captopril oxidation using voltammetry and amperometry was

investigated. The steps of fabrication for the Pt/NPGF electrode and oxidation of captopril at the surface of electrode are presented in Scheme 1.



Scheme 1. Schematic representation of the preparation of

Experimental

Chemicals

All of the used chemical reagent have analytical grade and were purchased from Merck (Darmstadt, Germany) unless otherwise is stated. Doubly distilled water was used throughout. A $1.0 \times 10^{-3} \text{ mol L}^{-1}$ captopril solution was prepared daily by dissolving 0.022 g captopril in water and the solution was

diluted to 100 mL with water. The solution was kept in dark at 4 °C. More dilute solutions were prepared by serial dilution with water. Phosphate buffer solution (PBS) was prepared by $\text{NaH}_2\text{PO}_4/\text{Na}_2\text{H}_2\text{PO}_4$ (0.1 mol L^{-1}) and desired pHs was adjusted by NaOH and HCl. Captopril tablets (DarouPakhsh Company, Iran, labeled 50 and 25 mg captopril per tablet) were

purchased from Red Cross Drug Store in Isfahan.

Apparatus

Cyclic voltammetry (CV), chronoamperometry and amperometry were performed using an electrochemical workstation (Autolab, PGSTAT302N). The used Cell in this study is made of Teflon, which is a conventional three-electrode cell assembly consisting of a platinum wire as an auxiliary electrode and an Ag/AgCl (KCl_{sat}) electrode as a reference electrode. Gold recordable compact disk (CD) was used as working electrode [24]. Thus a small piece of gold CD is cut and fixed to the bottom cell with an O-ring.

Scanning electron microscopy (SEM) was conducted using a Philips Model XLC microscope to characterize electrode morphology. A pH-meter (Corning, Model 140) with a double junction glass electrode was used to check the pH of the solutions.

Fabrication of platinum coated nanoporous gold film electrode

The used working electrodes throughout this work were constructed with small pieces of recordable disks (CD-R) made of gold [25, 26].

A typical NPGF electrode was prepared

using the method of reference [27]. The gold compact disk was cut into smaller pieces to produce substrates, which were secured to the bottom of a Teflon cell with an O-ring. The apparent electrode surface area was 0.28 cm². The NPGF electrode was prepared in two steps. Step one consisted of anodizing the gold substrate in a solution of 0.1 M phosphate buffer (pH = 7.2) for 3 min, applying a step potential from the open circuit potential (OCP) to 4.0 V vs. Ag/AgCl. Gas bubbles were produced from the gold surface during anodization. The growth of oxide film was accompanied by gas evolution at all times until anodization was terminated. Because only oxygen evolution can result in gas bubbles during anodic processing under these conditions, the bubbles produced at the anode must have been oxygen, even though no further detection was carried out. Afterwards, ascorbic acid was used as a nontoxic and inexpensive reducing agent to reduce gold oxide to metallic Au. The reduction was performed by incubating the anodized gold substrate in a solution of ascorbic acid (1.0 M) for 3 min. The color of the gold surface became dark due to its high surface area and nanometer crystal size [27]. The

Cu-decorated NPGF (CuNPGF) electrodes were constructed by immersing the NPGF electrode in a solution of 0.1 M H₂SO₄ containing of 1.0 mM CuSO₄.

Deposition of Cu was performed through stepping the electrode potential to a voltage at which Cu was underpotentially deposited (E_{UPD} , 0.25 V vs. Ag/AgCl). Then, the CuNPGF electrode was placed in a solution containing 5 mM H₂PtCl₆ in deaerated 50 mM HClO₄. The CuNPGF electrode was left in contact with the solution for 10 min at open circuit potential. The optimal immersion time has not been established in these experiments and an arbitrary time of 10 min has been adopted for all experiments. The electrode was then rinsed and the cell was filled with phosphate buffer. SEM and atomic force microscopy (AFM (BRUKER, Germany)) were used to characterize the morphology of the electrode.

Preparation of clinical samples

Urine samples (in a safe man without taking captopril) were stored in a refrigerator immediately after collection. Ten milliliters of the sample was centrifuged for 15 min at 1500 rpm. The supernatant was filtered using

a 0.45 μ m filter and then diluted 5-times with PBS (pH 7.2) [28, 29]. The solution was transferred into the voltammetric cell to be analyzed without any further pretreatment. Standard addition method was used for the determination of captopril in clinical samples.

Results and discussions

Characterization of PtNPGF electrodes

Typically, an NPGF electrode was prepared by anodic polarization of a gold film electrode in a phosphate buffer (pH= 7.2) under a chosen potential. The roughness factor of the NPGF electrode, defined as the ratio of the electrochemically active surface area to the geometrical area, was estimated from the cyclic voltammograms in 0.5 M H₂SO₄ solution by integrating the reduction charge of gold oxide monolayer [28, 29]. Figure 1 exhibits the curves of the smooth Au and NPGF electrodes in 0.5 mol L⁻¹ H₂SO₄ solutions.

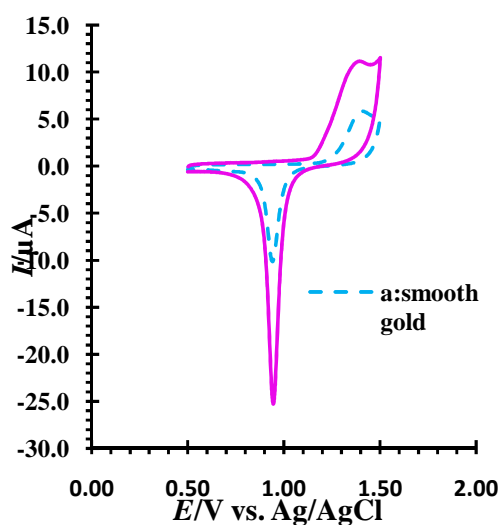


Figure 1. Cyclic voltammograms for (a) smooth gold electrode and (b) a NPGF electrode in $0.5 \text{ mol L}^{-1} \text{ H}_2\text{SO}_4$ at a scan rate of 50 mVs^{-1}

A voltammogram of smooth gold shows a symmetric cathodic peak at 0.93 V , resulting from the electrochemical reduction of gold oxide at positive potential scan. Cyclic voltammogram of NPGF electrode shows a similar electrochemical behavior with the smooth gold electrode except for the fact that both the anodic and cathodic peak currents increase substantially. The increase in peak current is resulted from the increased surface area of NPGF electrodes, and is thought possibly to reflect the nanoporous nature on the electrode surface. The apparent surface area of smooth gold was 0.380 cm^2 . The actual surface area is estimated

7.05 cm^2 for NPGF electrode that exhibits created porous in surface of NPGF electrode. Considering a specific charge of $386 \text{ } \mu\text{C}/\text{cm}^2$ required for gold oxide reduction [30], the roughness factor (ratio of apparent surface area over actual surface area) was determined 18.5 for NPGF electrode. This result supports effectiveness of the method involving in preparing a highly porous NPGF electrode. This result also provides strong evidence of an ultrahigh surface area of the NPGF electrode. Then, a Cu layer was deposited on the surface of NPGF electrode by UPD. Appropriate potential of UPD was estimated by CV of 5 mM CuSO_4 in $0.1 \text{ M H}_2\text{SO}_4$ solution on the NPGF electrode. Figure 2a shows electrochemical behavior smooth gold electrode at $5 \text{ mM CuSO}_4 + 0.1 \text{ M H}_2\text{SO}_4$ solution. The presence of two cathodic peaks a_1 and a_2 expressed the fact that deposition of Cu on smooth gold electrode occurs in two steps. The corresponding anodic peaks (b_1 and b_2) are observed on positive-going sweep. Peak a_1 is related to UPD Cu, where the monolayer of Cu deposit on the surface of smooth gold electrode and Cu overlayers deposit on Cu metal, peak a_2 shows OPD (over

potential deposition. The peak a_2 which is attributed to the bulk deposition of Cu imposes careful control of Cu UPD to avoid deposition of more than a monolayer of Cu.

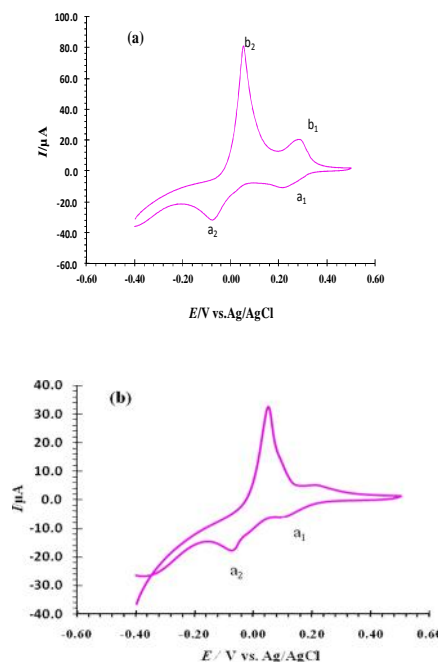


Figure 2. Cyclic voltammograms of (a) a smooth gold electrode and (b) a NPGF electrode in $0.1 \text{ mol L}^{-1} \text{CuSO}_4$ and $0.1 \text{ mol L}^{-1} \text{H}_2\text{SO}_4$ at a scan rate of 50 mVs^{-1}

This is critical since the amount of deposited Pt corresponds to the UPD Cu coverage. The voltammogram obtained in a repeated experiment using an NPGF electrode is shown in Figure 2b. Here, only two cathodic peaks (a_1 and b_1) which were observed are the same as the smooth gold electrode

(Figure 2a). This feature confirms the presence of the Cu at the surface of NPGF electrode after UPD. Afterwards, the prepared CuNPGF electrode was transferred to a solution containing Pt ($5.0 \times 10^{-3} \text{ mol L}^{-1} \text{H}_2\text{PtCl}_6$ in deaerated $5.0 \times 10^{-2} \text{ mol L}^{-1} \text{HClO}_4$). The electrode was left in this solution at open circuit

voltage for 10 min to ensure complete redox UPD Cu replacement and the resulting Pt ordering over layer [31].

The cyclic voltammogram of PtNPGF electrode was obtained after deposition of an ultrathin Pt layer on the NPGF electrode (Figure 3). This voltammogram shows an ascending feature due to Pt oxidation apparent from ~ 0.61 V in the positive scan direct, it leads to a sharp increase in current at anodic potential limit.

This feature clearly shows two step-like oxidation current for Pt with those of the latter located at less positive potential. The presence of a platinum oxide reduction peak at 0.3 V, along with a gold oxide reduction peak at 0.9 V become increasingly suppressed and shift to more positive potential in the negative scan direction, indicates the deposition of an ultrathin platinum layer on a NPGF electrode such that only a few gold site remain exposed. Such an electrochemical behavior has been reported previously for Pt in the literature [11]. The SEM and AFM images of NPGF and PtNPGF electrodes are shown in Figure 4.

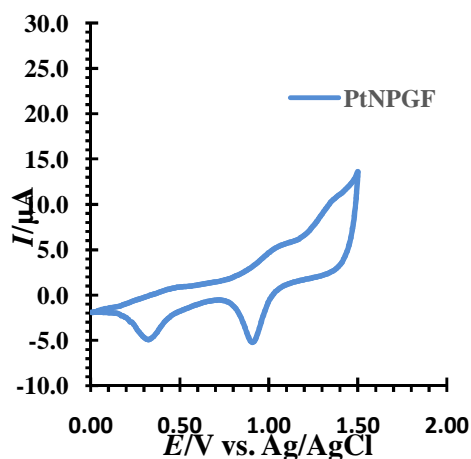


Figure 3. Cyclic voltammograms of PtNPGF electrode in $0.5 \text{ mol L}^{-1} \text{ H}_2\text{SO}_4$ at a scan rate of 50 mV s^{-1}

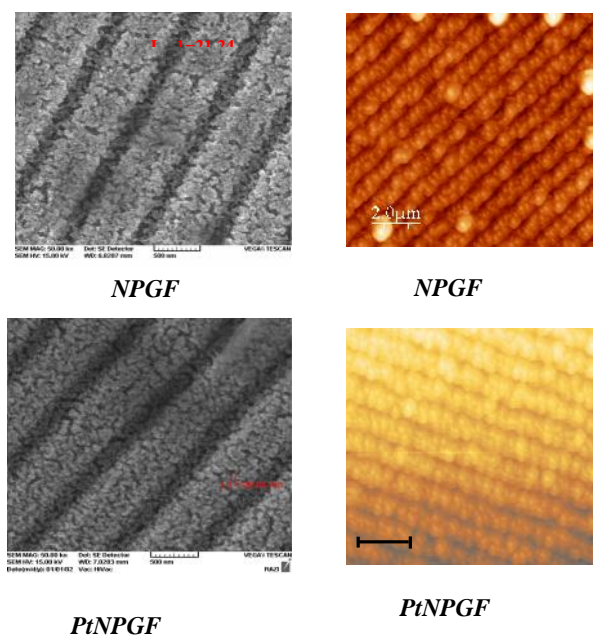


Figure 4. SEM and AFM images of surfaces NPGF and PtNPGF

Based on these figures it can be concluded that even after the UPD of copper and replacing the copper by Pt, the electrode porosity is preserved. Furthermore, a comparison between

particle size, defined on SEM images of NPGF and PtNPGF, indicates that the particle size of PtNPGF is larger than that of the NPGF. Also, their AFM images indicate that topography of PtNPGF is different from that of NPGF.

Electrooxidation of captopril on the PtNPGF

In order to investigate the electrocatalytic activity of the PtNPGF for electrooxidation of CAP, its cyclic voltammetric responses at scan rate of 50 mVs^{-1} were recorded in 0.1 mol L^{-1} PBS (pH 7.2) in the absence and presence of CAP (Figure 5).

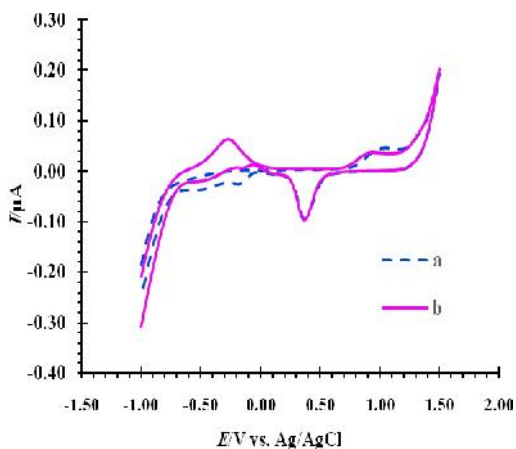


Figure 5. Cyclic voltammograms of (a) PtNPGF electrode with $\text{CAP}=5 \mu\text{mol L}^{-1}$, (b) NPGF electrode with $\text{CAP}=5 \mu\text{mol L}^{-1}$

Upon the addition of CAP, there was a drastic enhancement of the

anodic peak current at $\sim -0.2 \text{ V}$, without any cathodic peak for captopril, indicating an irreversible charge transfer in the system. Therefore, the data obtained clearly show that the combination of Pt and NPGF definitely improve the characteristics of the electrode for the oxidation of captopril. This voltammetric behavior can be shown an EC mechanism with a subsequent irreversible chemical reaction (dimerization of produced thiol radical) during the electro-oxidation of captopril. Thus, we proposed the following mechanism for the oxidation of captopril (RSH). The overall oxidative reaction process can therefore be attributed to the first initial electron, one proton oxidation of captopril (RSH) to generate the radical species RS which can undergo rapid dimerization to form the disulfide (RSSR) [4].

Assuming, many microholes and furrows were formed on the PtNPGF electrode surface so that the adsorption surface area was increased, this would then explain the increase could in peak current. Of course, this increase has also resulted from the good electrical communication between the Pt film and the NPGF and synergistic effect.

Nanosized platinum has long been used to catalyse the oxidation of CAP. Herein, the nanoporous morphology of platinum nanofilm also exhibited fascinating catalytic activity by increasing the oxidation current. The major factor for its excellent catalytic property may be attributed to the high surface energy resulting from the surface effect of the nanoparticles. On the obtained platinum nanofilm electrode, the surface roughness and surface area were increased, corresponding to the formation of many nanometer-sized platinum particles. Compared with bulk platinum, the platinum nanofilm exposes more active sites with high surface energy, which facilitates the oxidization of CAP.

To illustrate the special effects of the PtNPGF catalyst towards the oxidation of CAP, the characteristics of the oxidation of CAP at smooth gold film, NPGF, CuNPGF, and smooth Pt electrodes in 0.1 mol L⁻¹ phosphate buffer (pH 7.2) containing 5 μmol L⁻¹ CAP were compared with those obtained at the PtNPGF electrode. The results obtained are shown in Figure 6.

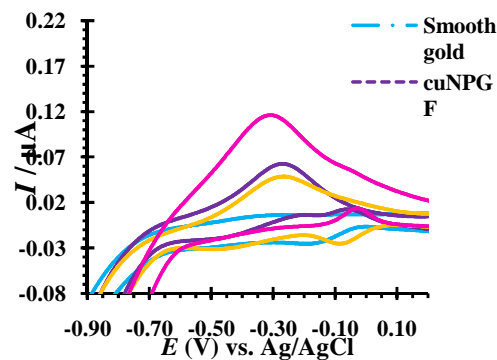


Figure 6. Cyclic voltammograms of 5 μmol L⁻¹ CAP solution in PBS 0.1 mol L⁻¹ (pH 7.2), at a scan rate of 50mVs⁻¹ on smooth gold film(GF) , NPGF, CuNPGF and PtNPGF electrodes

However, by carefully analyzing the curves in Figure 6, it is obvious that the electrocatalytic current at PtNPGF is approximately 17 times of that obtained at the smooth gold electrode and 2 times of that obtained at the NPGF electrode. The electrocatalytic features of these electrodes are similar to those of the PtNPGF electrode. These results demonstrate that the electrocatalytic activity of the PtNPGF electrode is much higher than that of NPGF, CuNPGF, smooth gold and bulk Pt electrodes. Meanwhile, the peak potential of CAP obtained at the NPGF has also shifted to be more than 80 mV in comparison with that at the PtNPGF. The electrocatalytic activity of PtNPGF can be considered to result from the catalytic activity of the Pt nanostructures, good electrical

communication between the Pt film and the NPGF, and synergistic effects.

Moreover, the voltammetric results indicated that the bulk Pt electrode lost its electrocatalytic activity quickly due to the accumulation of chemisorbed intermediates, which blocked the Pt electrode surface. The results reveal that the electrocatalytic oxidation of CAP at the surface of the PtNPGF catalyst is effective and the electrocatalytic activity of PtNPGF is much higher than that of bulk Pt catalyst.

It is widely reported that the activity of thin film catalysts depends on the physicochemical properties of the substrate and may be drastically different from that of the corresponding bulk material [32]. Similarly, the reactivity and adsorption at metal thin films can be described by the shift of the d-band center energy. According to Nørskov et al. [33], the characteristics of the surface metal d-bands, particularly the weighted center of the d-band, play a decisive role in determining surface reactivity. When a thin Pt layer is deposited on gold surface, there is an upper shift in d-band center to maintain a constant filling of the d-band, which leads to a

higher adsorption energy of the adsorbents such as oxygen containing species. Two factors contribute to the change in the metal overlayer d-band center energy: the electronic coupling between the Pt overlayer and its substrate (ligand effect) and the strain (geometric effect) [34]. By increasing the Pt coverage on the Au substrate, both of these effects become weaker, hence, the Pt oxide reduction peak shifts to more positive potentials. Therefore, the Au support could provide a promotional effect on the catalytic activity of Pt overlayers, the extent of which depends on the nature of the substrate and thickness of the catalyst overlayer.

To figure out the reaction mechanism of CAP on the surface of PtNPGF electrode, scan rate dependent experiments were carried out and the results are shown in Figure 7. In pH 7.2 PBS, the anodic peak currents of CAP are proportional to the square root of the scan rate in the range of 3–50 mVs^{-1} , indicating that the process is diffusion rather than surface controlled (Figure 7 a). As the potential sweep rate increased, the oxidation peak potentials shifted to more positive values, confirming the limitation of the kinetics

of the electrochemical reaction (Figure 7 b). The Tafel plot was also investigated from the data taken from the rising part of the current –voltage curve recorded at a scan rate of 5 mV s^{-1} . This part of the voltammogram, known as a Tafel region is affected by the electron transfer kinetics between the CAP and the electrode surface. Under this condition, the number of electron involved in the rate determining step can be estimated from the slope of the Tafel plot. A slope of 0.8938 V/decade was obtained, indicating a one- electron transfer to be rate limiting. A transfer coefficient of $\alpha = 0.45$ was obtained which was in good agreement with literature [33].

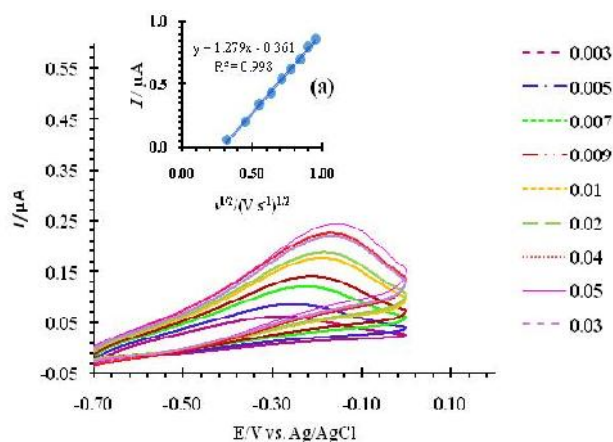


Figure 7. a) The plot of anodic peak currents of PtNPGF electrode vs. $v^{1/2}$ from the cyclic voltammograms of $5 \mu\text{mol L}^{-1}$ CAP b) Current–potential curve for electrooxidation of $5 \mu\text{mol L}^{-1}$ CAP at the surface of PtNPGF electrode at various scan rate in PBS, 0.1 M, pH

The effects of pH on the peak potential and peak current of $5 \mu\text{mol L}^{-1}$ captopril in 0.1 molL^{-1} PBS at different pHs in the range of 2-9 were investigated. A cathodic shift in anodic potential peak is occurred by increasing of the pH of buffer solution. The calibration curve of E versus pH, in the pH range of 4.0-7.6, has the slope of -48.9 mVpH^{-1} and in other pHs deviates from linear. With respect to loss of an electron in the electro oxidation of captopril, contribution of a proton is suggested in the electrode reaction. It was also found that the electrocatalytic oxidation of CAP at the surface of PtNPGF was more favored under neutral conditions than in acidic or basic medium. Thus the pH 7.20 was chosen as the optimum pH for electrocatalysis of CAP oxidation at the surface of PtNPGF.

Amperometry sensing of captopril

To find the optimal conditions for the amperometric sensing of captopril, the effect of applied potential on the response current of the sensor was investigated. Figure 8 shows the dependence of sensitivity of the PtNPGF electrode in 0.1 M PBS (pH 7.2) with $5 \mu\text{mol L}^{-1}$ CAP at applied potentials of 0.25-0.75 V. The best

result in terms of sensitivity and signal-to-noise ratio was obtained at $E = -0.25V$, thus this potential was chosen for evaluation of sensing properties of our electrode.

The amperometric response of the PtNPGF electrode to CAP is measured by successive addition of $5 \mu\text{mol L}^{-1}$ captopril in 0.1 mol L^{-1} PBS (pH 7.2) at a fixed potential of $-0.25V$.

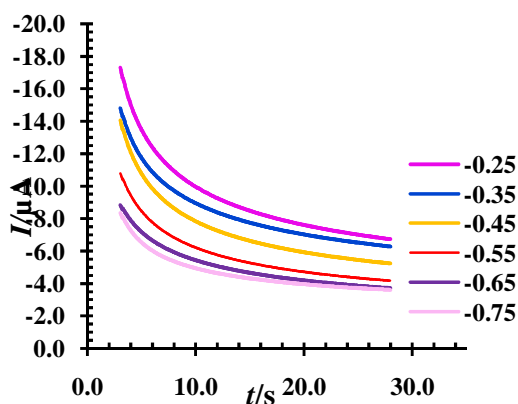


Figure 8. The effect of potential on current of $5 \mu\text{mol L}^{-1}$ CAP at the surface of PtNPGF electrode in PBS 0.1 mol L^{-1} at a scan rate of 50 mV s^{-1}

The obtained current versus time in Figure 9 (a) shows that the time required to reach 95% of the steady state value is less than 10 s after addition of captopril. From the calibration curve for CAP in Figure 9 (b), it is clear that the current is linear to captopril concentration in the range $4.70 \times 10^{-8} - 4.57 \times 10^{-5} \text{ mol L}^{-1}$, with regression equation $y \text{ (mA)} =$

$0.0477 \pm 0.0020 C_{\text{CAP}} \text{ (mmol L}^{-1}) + 0.325 \pm 0.050$ and correlation coefficient of 0.9986 ($n=10$). The detection limit is estimated to be $1.2 \times 10^{-8} \text{ mol L}^{-1}$ at a signal to noise ratio of 3. A performance comparison of this sensor with other captopril sensors is summarized in Table 1 and shows the PtNPGF electrode have excellent electrocatalytic activity toward captopril detection, and a good performance in the direct estimation of captopril at a low applied potential of -0.2 V , thus avoiding the problematic interference from ascorbic acid and uric acid.

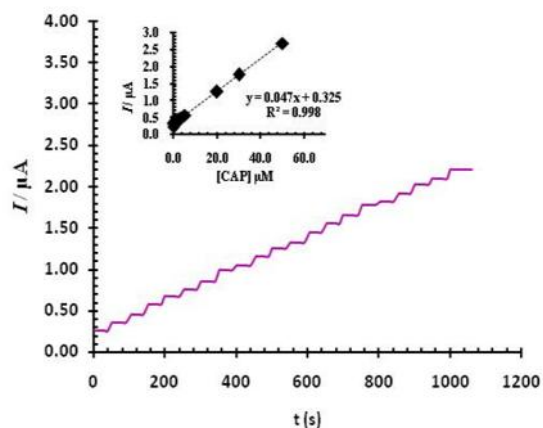


Figure 9. a) Amperometric responses of CAP on the PtNPGF electrode at -0.25 V vs. Ag/AgCl upon successive additions of $20 \mu\text{mol L}^{-1}$ CAP, b) Calibration curve with different concentration of CAP PtNPGF electrode (PBS, 0.1 M , pH 7.2).

Table 1. Comparison of the efficiency of some methods in the determination of captopril

Electrode	Methods	Linear range (μM)	Detection limit (μM)	Peak potential (mV)	Reference
CPE	Square wave voltammetry	0.3 to 140	0.090	490	[35]
CPE	Cyclic voltammetry	4.0 to 110	1.10	650	[4]
CPE	Cyclic voltammetry	0.8 to 65	0.30	470	[36]
PtNPGF	Amperometry	0.046 to 47	0.012	-200	This Work

^a Average of five replicate measurements

Reproducibility and stability of the PtNPGF sensor

Reproducibility and long-term stability are major requirements for long-lasting sensor application. The repeatability of the PtNPGF electrochemical sensor was measured in 0.1 mol L^{-1} PBS (pH 7.2) under hydrodynamic conditions.

Repeated use of the electrode did not affect its performance. In a series of 10 successive measurements, $5 \text{ } \mu\text{mol L}^{-1}$ CAP was measured continuously, and a good repeatability with a relative standard deviation (RSD) of 2.4% was obtained. The reproducibility of the CAP sensor was evaluated by the comparison of the currents generated by different electrodes prepared under the same conditions. The amperometric response of 5 PtNPGF electrodes to $5 \text{ } \mu\text{mol L}^{-1}$ CAP was examined, providing a relative standard deviation (RSD) value of 3.1%.

The long-term stability of the CAP sensor electrode was followed by measuring the response to $5 \text{ } \mu\text{mol L}^{-1}$ CAP. The electrode was stored in air at room temperature ($25 \pm 1^\circ\text{C}$) when not in use. The response was found to remain at 99.0% of its original response after 7 days, and 96.2% after 20 days. Even after a prolonged storage (50 days), the electrode retained 92.5% of its initial response, indicating good long-term stability. Excellent stability and reproducibility indicated that the catalyst layer on the electrode's surface was structurally stable, free from morphological changes, and not significantly affected by repeated measurements under rigorous conditions.

Determination of CAP in biological samples

To investigate the applicability of the proposed sensor for the catalytic

determination of captopril in clinical samples, we selected urine sample for the analysis of their captopril contents. The urine sample was centrifuged and diluted five-times with buffer solution without any further pretreatment. The standard addition method was used for measuring captopril concentrations in the samples. The results demonstrated

the capability of PtNPGF for voltammetric determination of captopril in clinical samples with good recoveries of the spiked captopril and good reproducibility (Table 2).

Table 2. Determination of captopril in human urine samples

Sample	Added (μM)	Expected (μM)	Found ^a (μM)	R.S.D. (%)	Recovery (%)
urine	0	-	< detection limit	-	
urine	10	10	10.07 \pm 0.45	2.23	99.9
urine	20	20	20.14 \pm 0.63	2.52	101
urine	30	30	29.94 \pm 0.99	2.62	99.8

Interference Studies

Some substances existed in biological samples could interfere with the detection of captopril. The influence of foreign compounds that can be found in typical biological samples containing CAP was investigated by using solutions containing 50.0 $\mu\text{mol L}^{-1}$ captopril at pH 7.2 and various concentrations of the interfering compounds. The potentially interfering substances were chosen from the group of compounds commonly found with captopril in biological fluids and in pharmaceuticals. Tolerance limit was

defined as the maximum concentration of the interfering substance that caused an error less than $\pm 5\%$ for the determination of captopril. The results showed that 950-fold of glucose, sucrose, ascorbic acid and uric acid; 900 fold of Na^+ , K^+ , Ca^{2+} , Mg^{2+} and NH_4^+ , 500-fold of atenolol, prazosin, hydrochlorothiazid did not affect the selectivity.

Conclusion

The preliminary data presented in the present paper indicate that the fabricated PtNPGF electrode has a significant catalytic activity towards the

CAP. The platinum loading of this electrode is very low and its activity is better than a NPGF electrode. The PtNPGF electrode has the best electrocatalytic activity towards captopril oxidation reaction, which could be related to a good electrical communication between the Pt and the NPGF and synergistic effect.

Thus, the excellent electroanalytical performance as a result of combined advantages of low working potential with larger sensitivity, good reproducibility, acceptable long-term stability, high selectivity and simple preparation procedure implies that the PtNPGF can provide an efficient and new sensor with minimal use of precious metal components. Finally, the mechanical stability of as-fabricated electrode and relatively high current of captopril oxidation, makes it a potential candidate for determination of captopril.

Acknowledgements

The authors gratefully acknowledge financial support of the Research Council of Payame Noor University.

References

- [1] N. Aykin, R. Neal, M. Yusof, N. Ercal, *Biomed. Chromatogr.*, **2001**, *15*, 427-432.

[2] A.M. Pimenta, A.N. Araújo, M.C.B. Montenegro, *Anal.Chim.Acta*, **2001**, *438*, 31-38.

[3] W. Siangproh, P. Ngamukot, O. Chailapakul, *Sens. Actuators, B*, **2003**, *91*, 60-66.

[4] S. Shahrokhian, M. Karimi, H. Khajehsharifi, *Sens. Actuators, B*, **2005**, *109*, 278-284.

[5] A. Wong, M. RvLanza, M. Dpt Sotomayor, *Comb. Chem. High Throughput Screening*, **2010**, *13*, 666-674.

[6] B. Rezaei, S. Damiri, *Sens. Actuators, B*, **2008**, *134*, 324-331.

[7] H. Karimi-Maleh, M. Moazampour, V.K. Gupta, A.L. Sanati, *Sens. Actuators, B*, **2014**, *199*, 47-53.

[8] M. El Reis, F. AbouAttia, I. Kenawy, *J. Pharmaceut. Biomed.*, **2000**, *23*, 249-254.

[9] R. Haggag, S. Belal, R. Shaalan, *Sci. Pharm.*, **2008**, *76*, 33.

[10] F. Pogacean, A.R. Biris, M. Coros, M.D. Lazar, F. Watanabe, G.K. Kannarpady, S.A.F. Al Said, A.S. Biris, S. Pruneanu, *Int. J. Nanomed.*, **2014**, *9*, 1111.

[11] P. Liu, X. Ge, R. Wang, H. Ma, Y. Ding, *Langmuir*, **2008**, *25*, 561-567.

[12] F. Jia, C. Yu, K. Deng, L. Zhang,

- J. Phys. Chem. C*, **2007**, *111*, 8424-8431.
- [13] J.H. Shim, J. Kim, A. Go, C. Lee, Y. Lee, *Mater.Lett.*, **2013**, *91*, 330-333.
- [14] K. Sasaki, J. Wang, H. Naohara, N. Marinkovic, K. More, H. Inada, R. Adzic, *Electrochim.Acta*, **2010**, *55*, 2645-2652.
- [15] V. Stamenkovic, B.S. Mun, K.J. Mayrhofer, P.N. Ross, N.M. Markovic, J. Rossmeisl, J. Greeley, J.K. Nørskov, *AngewandteChemie*, **2006**, *118*, 2963-2967.
- [16] S.-E. Bae, D. Gokcen, P. Liu, P. Mohammadi, S.R. Brankovic, *Electrocatalysis*, **2012**, *3*, 203-210.
- [17] Z. Huang, Q. Xie, Y. Tan, S. Huang, J. Huang, Y. Meng, S. Yao, *Sci. China: Chem.*, **2010**, *53*, 2349-2356.
- [18] R.R. Adzic, J. Zhang, K. Sasaki, M.B. Vukmirovic, M. Shao, J. Wang, A.U. Nilekar, M. Mavrikakis, J. Valerio, F. Uribe, *Top. Catal.*, **2007**, *46*, 249-262.
- [19] A.M. Prasad, C. Santhosh, A.N. Grace, *Appl. Nanosci.*, **2012**, *2*, 457-466.
- [20] S.y. Huang, C.m. Chang, K.w. Wang, C.t. Yeh, *ChemPhysChem*, **2007**, *8*, 1774-1777.
- [21] N.M. Markovi, H.A. Gasteiger, C.A. Lucas, I.M. Tidswell, P.N. Ross Jr, *Surf. Sci.*, **1995**, *335*, 91-100.
- [22] H.-G. Choi, P.E. Laibinis, *Anal. chem.*, **2004**, *76*, 5911-5917.
- [23] E. Herrero, L.J. Buller, H.D. Abruna, *Chem. Rev.*, **2001**, *101*, 1897-1930.
- [24] A. Kiani, E.N. Fard, *Electrochim.Acta*, **2009**, *54*, 7254-7259.
- [25] L. Angnes, E.M. Richter, M.A. Augelli, G.H. Kume, *Anal. chem.*, **2000**, *72*, 5503-5506.
- [26] F. Jia, C. Yu, J. Gong, L. Zhang, *J. Solid State Electrochem.*, **2008**, *12*, 1567-1571.
- [27] Y. Deng, W. Huang, X. Chen, Z. Li, *Electrochem. Commun.*, **2008**, *10*, 810-813.
- [28] N. Tavakkoli, S. Nasrollahi, G. Vatankhah, *Electroanalysis*, **2012**, *24*, 368-375.
- [29] N. Tavakkoli, S. Nasrollahi, *Aust. J. Chem.*, **2013**, *66*, 1097-1104.
- [30] R. Szamocki, A. Velichko, C. Holzappel, F. Mücklich, S. Ravaine, P. Garrigue, N. Sojic, R. Hempelmann, A. Kuhn, *Anal. chem.*, **2007**, *79*, 533-539.
- [31] E. Rouya, S. Cattarin, M. Reed, R. Kelly, G. Zangari, *J. Electrochem. Soc.*, **2012**, *159*, K97-K102.
- [32] J. Zeng, J. Yang, J.Y. Lee, W. Zhou, *J. Phys. Chem. B*, **2006**, *110*, 24606-24611.

- [33] J. Greeley, J.K. Nørskov, M. Mavrikakis, *Annu. Rev. Phys. Chem.*, **2002**, 53, 319-348.
- [34] J. Kitchin, J.K. Nørskov, M. Barteau, J. Chen, *J. Chem. Phys.*, **2004**, 120, 10240-10246.
- [35] H. Karimi-Maleh, A.A. Ensafi, A. Allafchian, *J. Solid State Electrochem.*, **2010**, 14, 9-15.
- [36] M.A. Khalilzadeh, H. Karimi-Maleh, A. Amiri, F. Gholami, *Chin. Chem. Lett.*, **2010**, 21, 1467-1470.